Larval Fish Transport Dynamics in an arid Estuary do not follow Selective Tidal Stream Transport Mechanisms

Hans Sloterdijk*, [a, b], Patrice Brehmer *,[d, f] Ibrahima Ndiaye [d,e,f], Xavier Capet [c], Werner Ekau [b]

[a] Christian-Albrechts-University Kiel, Center for Ocean and Society (CeOS), Germany
[b] Leibniz Centre for Tropical Marine Research (ZMT) GmbH, Bremen, Germany
[c] LOCEAN Laboratory, CNRS-IRD-Sorbonne Universités, UPMC, MNHN, Paris, France
[d] IRD, Univ Brest, CNRS, Ifremer, Lemar, CSRP, BP 1386, Hann, Dakar, Senegal
[e] Université Cheikh Anta Diop de Dakar, Institut Fondamental d'Afrique Noire, IFAN, Département de biologie animale, Dakar, Senegal
[f] Institut Sénégalais de Recherches agricoles, ISRA, Centre de Recherches Océanographiques de Dakar-Thiaroye, CRODT, PRH, BP 2241, Dakar, Senegal

*Corresponding authors: Patrice Brehmer, E-mail: patrice.brehmer@ird.fr; Hans Sloterdijk, E-mail: hsloterdijk@kms.uni-kiel.de

Abstract

The mechanisms governing larval fish transport between low-flow estuaries and coastal waters in seasonally arid climates remain poorly understood. To address this, we conducted a field study in the Sine Saloum Estuary, a tropical inverse estuary in West Africa. We used simultaneous measurements of current profiles and larval fish densities during semi-diurnal tidal cycles at three strategic locations. We focused on economically and ecologically important fish families (Clupeidae, Cynoglossidae, Gerreidae, and Mugilidae) known for their contrasting life histories and reliance on estuarine environments. The estuarine system was characterized by inverse salinity gradients, partial stratification, and gravitational circulation, offering natural pathways for larval retention. Unlike traditional estuarine systems, no evidence of selective tidal stream transport (STST) was found; instead, fish larvae exhibited stable depth preferences independent of diel and tidal cycles. This simpler mechanism, requiring minimal energy expenditure, appears to rely on gravitational circulation for effective larval transport. The prevalence of the gravitational circulation and the low energy cost for larvae to maintain themselves over a defined depth range vs the desired direction of mean displacement make the proposed larval transport mechanism potentially important most of the year. These findings provide critical insights into the biological and physical processes shaping larval fish recruitment in arid estuarine systems and emphasize the need for adaptive management strategies to support fisheries under changing environmental conditions.

Keywords: estuarine circulation, larval recruitment, larval transport, ichthyoplankton transport, tidal transport, fish larvae, Saloum Delta, inverse estuary.

1. Introduction

Fish are particularly vulnerable to ecological and environmental challenges during their early life stages. Underlining its significance for the fates of year classes (Hjort, 1926), most species suffer high mortality during this period (May 1974). Most marine fishes have non-swimming or weakly swimming pelagic early life stages. Thus, fish larvae have locomotion capabilities that differ drastically from those of larger juvenile and adult fishes (Brehmer et al., 2011b). Accordingly, the distribution of larval fishes is at least partially controlled by passive transport mechanisms (Norcross and Shaw, 1984). The term “larval transport” describes the movement of fish larvae in the marine environment (Pineda et al., 2007). At first, the transport of larvae in coastal areas is largely due to passive advection by oceanographic processes such as wind-driven circulations, convergence flows near river fronts, internal waves, tidal currents, net currents, river plumes, upwelling or downwelling currents, and eddies, which all can vary on a broad range of scales, from yearly, seasonally, daily, hourly, and down to a few minutes (Teodósio et al., 2016). Under unfavourable flow conditions, fish larvae might be transported to habitats less suitable for development, where they may fail to find appropriate amounts and types of planktonic prey (Hjort, 1914, 1926) or survive the prevailing abiotic conditions concerning, for instance, temperature, salinity, dissolved oxygen, or UV-radiation (Miller and Kendall, 2009).

Many inshore marine fishes in temperate and tropical environments spawn offshore. Their larvae or juveniles use shallow habitats such as bays, mangroves, and other estuarine regions as nurseries (Beck et al., 2001) before moving and returning to adult habitats. Such life history pattern was often observed in commercially and recreationally important fish species (Haedrich, 1983). Hence, larval transport has central implications for recruitment, as the maintenance of marine populations often depends on the completion of larval migration from the open ocean spawning regions to estuarine nursery habitats. Limitedly understood, but a critical stage of this journey is ingress, retention, and movement between the coastal waters and an estuary (Churchill et al., 1999).

Most estuaries present special challenges to larval transport for marine taxa using them because their waters experience net seaward motion, and current velocities frequently exceed larval swimming speeds (Boehlert and Mundy, 1988; Forward Jr et al., 1999; Brehmer et al., 2011a). Nevertheless, for some species, postflexion larvae can out-swim currents in nurseries and even recruit against ebbing tides (Pattrick and Strydom, 2009). Different larval transport and resulting recruitment problems related to estuarine use have been identified among fish species. First, some species are resident in estuaries throughout their life histories, and their primary recruitment problem is to prevent the export of their early life stages from the estuary. Second, other species that visit estuaries periodically as adults for spawning face the same export problems as the residents. Finally, species that spawn offshore and subsequently enter estuarine systems as larvae or early juveniles face challenges of ingress to the estuarine nursery areas and preventing export once they have entered. An important question, therefore, is how such larvae, with their limited swimming capabilities, move in or out of these nursery areas.

Theoretically, larval transport can be influenced by several elements of estuarine circulation. The dominant sources of water circulation in estuaries are tides, river flows, winds, non-tidal forcing from the coastal ocean, and topographically induced circulations (Norcross and Shaw, 1984). In most estuaries, the general pattern of circulation (“two-layer estuarine circulation”) is an outflow near the surface that is partially balanced by a net inflow in the bottom layer (Dyer, 1997). Accordingly, larval vertical behaviour can also modify and feasibly control the movement of larvae into an estuary(Melville-Smith et al., 1981; Pattrick and Strydom, 2014). There has been a long history of investigating larval transport of fishes in stratified estuaries that experience substantial freshwater input and the most commonly cited behavioural mechanism leading to up-estuary movement by larvae is selective tidal stream transport (STST), in which larvae are up in the water column during rising tides and low in the water column during falling tides (Boehlert and Mundy, 1988; Forward Jr et al., 1999; Weinstein et al., 1980). STST has been the suggested mechanism for movement and retention within estuaries in several fish species, such as young anguillid eels, herrings, shads, croakers, and plaice (McCleave and Kleckner, 1982; Tanaka et al., 1989; Fukuda et al., 2016; Weinstein et al., 1980). However, STST is constrained to certain hydrodynamic boundaries (Forward and Tankersley, 2001).

In semi-arid climates, where rainfall is extremely low and insufficient to stratify estuaries during most of the year, the density of the water at the estuary's mouth is often similar to that in the ocean, and tidal diffusion rather than "two-layer estuarine circulation" may control exchange between the estuary and the open coast (Largier et al., 1997; Nidzieko and Monismith, 2013). However, excess evaporation over wide coastal or estuarine areas can also produce inverse salinity gradients pointing toward the head of the water body, partially stratified conditions, and a reverse thermohaline circulation with the bottom outflow of salty water. This has been observed in many parts of the (sub)-tropics (Nunes Vaz et al., 1990; Lavín et al., 1998; Hetzel et al., 2013).

This study focuses on understanding hydrography and the implications of physical dynamics on the potential pathways for larval fish transport at the interface of a tropical estuary connected to the North Atlantic Ocean. Over the past decades, the Sine Saloum Estuary (Senegal) has been particularly affected by precipitation deficits combined with intense evaporation. This has resulted in a more extreme and prevalent low-flow regime and increasing overall salinity (Simier et al., 2004; Xenopoulos et al., 2005; Mbow et al., 2008). What is currently unidentified is how these changes affect the physical and behavioural processes mediating larval transport between the estuarine waters and the open coast. These changes could affect fisheries locally and regionally, and the impacts have the potential to be an issue, especially in developing countries where the economic and social systems are greatly dependent upon their fisheries. The input of fish larvae is one factor determining the importance of an estuary for many commercially important fish species. A better understanding of these physical and biological mechanisms will allow us to assess the impact of such environmental changes.

The sampling scheme in this study was designed to test whether fish larvae utilized tidal currents (ebb and flood) for their upstream or downstream transport in the estuary, and if so, whether the larvae predominantly entered the estuary in a specific location across the estuary (Brehmer et al., 2006). In the context of climate change and the increasing number of estuaries in arid and semi-arid areas, it becomes important to test the STST mechanism in this particular context. Understanding these mechanisms could help mitigate the adverse effects of environmental changes on fish populations and support the sustainable management of estuarine ecosystems and the fisheries they support.

2. Materials and Methods

This study first examined the flow structure at the entrance of the Saloum branch of the Sine-Saloum Estuary. Second, it focused on the movement of fish larvae in and out of the estuary by analyzing variations in larval fish densities and transport in relation to the tidal phase, time of day, and location within the entrance of the Saloum River branch. Lastly, it emphasized the impact of larval behaviour and other biological mechanisms by which larval fishes are transported between coastal waters and estuarine areas.

2.1. Study system: the Sine Saloum inverse estuary

Situated in Senegal, West Africa (13°30’-14°30’ N, 16°00’-16°80’ W), the Sine Saloum system (**Fig. 1a**) is representative of estuaries that receive, except from seasonal local rainfall, little or no freshwater input. Under intense evaporation, their upper reaches have become highly saline and hypersaline. Between 1951 and 1980, the average yearly precipitation in the Sine Saloum Estuary ranged from 880 mm in the southern part to 480 mm in the northernmost part (Dacosta, 1993). The average 828 mm recorded in the fifties (Diaw et al., 1993) is now only about 500 mm, with rains concentrated over 3-4 months and surrounded by prolonged drought periods. This recorded change in the precipitation rate corresponds to a deficit of about 10 billion m^3 of freshwater input (Diouf, 1996). Classified as an inverse estuary (Pritchard, 1967), throughout the year, salinity ranges from 35 to 41 at the sea mouth and can reach over 130 in the upstream areas.

This study was conducted at the mouth of the Saloum branch of the Sine Saloum Estuary (**Fig. 1a**). The Saloum entrance connects the Tropical Atlantic Ocean to the estuarine areas at an average depth of 10 m and extends in a south-north direction over approximately 3 km (**Fig. 1b**). The west side of the entrance is bordered by a sand spit (Pointe de Sangomar). In contrast, the east side is bordered by patchy mangrove cover. The average width of this reach is 1.5 km. Regional tides are semi-diurnal, having an average tidal amplitude of about 1.20 m. The Saloum region is economically based on fishing activities and marine conservation (Thiaw et al., 2021).

2.2. Hydrodynamics and physicochemical sampling

2.2.1. Hydrodynamic data acquisition

Vertical current profiles (speed and direction) and bottom pressure were measured continuously over approximately 2.5 semi-diurnal tidal cycles at three locations at the entrance of the Saloum branch of the Sine-Saloum Estuary (**Fig. 1**). ADCPs were deployed on 09 July 2014 for about 30 hours, starting at 09:00 UTC (Coordinated Universal Time, which is local time) and ending on 10 July 2014 at 15:00 UTC. Three upward-looking Acoustic Doppler Current Profilers (ADCPs) fastened to the base of aluminium frames were deployed and anchored on the sea floor (bottom mounted) with approximately uniform spacing across the channel's western and eastern flanks and near the centre, forming a transect line perpendicular to the entrance (**Fig. 1b**). These locations were named West, Centre, and East (**Table A1** in **Appendix 1**). As it is standard procedure for ADCP's data, near-surface data were discarded because of contamination from echoes scattered back from the sea surface (the depth above which data were considered non-usable was determined objectively; see *Section 2.4.1*). Near-bottom data are also unavailable because of the depth of the instrument head (~ 0.5 m above ground) and the additional blanking distance. Consequently, the "West-Centre-East" deepest measurement cells were centred at 1.1, 2.0 and 1.5 m above the sea floor, respectively.

Despite being part of the climatological monsoon season, no major rainfall occurred in the months before our observational period, characterized by the absence of freshwater run-off in the Sine Saloum Estuary. Thus, our observations represent the warm and dry conditions preceding the monsoon onset. It also followed the seasonal maximum larval abundances observed in a previous study (Sloterdijk et al., 2017). The tidal amplitude was close to average, with a forecasted tide coefficient of 72. Weather conditions during the survey were fair, with winds consistently below 10 knots.

2.2.2. Physicochemical data acquisition

One shallow water boat (Diassanga, 10m, IRD) was used to sample the West (W), Centre (C), and East (E) locations. Salinity (psu), water temperature (°C), and dissolved oxygen (mg l^{-1}) were measured using a portable multi-parameter field instrument (WTW Multi 3430®). Vertical profiles of the physico-chemical variables were obtained by taking measurements starting at the surface with depth intervals of one meter until the bottom was reached. Measurements of each location occurred at approximately 2-hour intervals and coincided with larval sampling. Additionally, salinity measurements acquired during other field campaigns (Sloterdijk et al., 2017) (November 2013, February, June, and August 2014) at locations along the Saloum branch of the Sine Saloum Estuary were used in this study to assess bottom and surface longitudinal salinity differences between pre-established sectors (**Fig. 1a**; downstream, midstream, and upstream) as a function of the season.

2.3. Biological data acquisition: Fish larvae sampling

Fish larvae were actively sampled at each location at approximately 2-hour intervals. Two types of nets, both with a mesh size of 500 µm were used: a paired neuston net (opening 30 x 15 cm, 3 m long) stacked on top of each other for collecting fish larvae at and near the surface and a ring trawl (ø 0.60 m, 3 m long) to collect fish larvae in the water column. Accordingly, three strata were sampled and referred to as Surface (Neuston Top), Near Surface (Neuston Bottom), and Mid-Water (Ring Trawl). Both nets were custom-made to be operated from an adapted catamaran (Hobie Cat 15®) that was deployed alongside a towing boat (R/V Diassanga), ensuring larval sampling was conducted well clear of its bow wave and wake. Each sample consisted of a 5-minute horizontal haul in the direction of the current at an average speed of 2-3 knots. The same nets and fishing efforts were deployed in each location.

The volume of water filtered was calculated using mechanical flow meters (Hydro-Bios®) attached to the centre of the nets so the number of larvae caught could be standardized into the number of larvae per m^3 for density measurements. Samples were immediately preserved in 30 % alcohol/seawater and stored and cooled in an on-board electric coolbox. Fish larvae were sorted from the catches in the laboratory and gradually transferred to 50 and 70 % alcohol. In addition, standard length (SL) to the nearest 0.01 mm (measured from the tip of the snout to the end of the notochord (Miller and Kendall, 2009)) was measured for all larvae at each sampling location. Collected specimens were identified to the lowest possible taxon using traditional morphological techniques (Tamoikine and Pandare, 1994; Moser, 1996; Leis and Carson-Ewart, 2004; Richards, 2006). Due to the paucity of original descriptions and illustrations of fish larvae in the literature covering the area of interest, the smaller individuals could not always be identified at the species or genus level but only at the family level. Accordingly, a selection of the four most abundant taxa in the samples was made, and further analysis in this study concentrated on Clupeidae, Cynoglossidae, Gerreidae, and Mugilidae larvae.

2.3.1 Ethics Statement

This study does not involve human subject research, experiments on animals, or the use of anesthesia, euthanasia, or any form of animal sacrifice. Field research activities were conducted with proper authorization, as permission was granted by the Institut de Recherche Agricoles Senegalais (ISRA). All research practices comply with ethical standards and relevant regulations.

2.4. Data analyses

2.4.1. Water current data processing

In a stratified estuary, velocities (v) are expected to differ between the surface and the bottom. This may have important implications because near-passive organisms such as eggs and larvae can modulate their lateral transport by modifying their position in the water column, *e.g.*, through buoyancy or vertical migration adjustments.

To quantify this effect, we aimed to compute the vertical velocity shear at the mooring locations using the following equation:

$$\delta v(t) = v(surface) - v\,(bottom) \qquad \text{(Eq. 1)}$$

However, due to limitations of the ADCP, these velocities were not directly available. Instead, they were computed using the indices $n_{up}$and n_{lo}, representing the uppermost and lowermost valid measurement cells, respectively, where ADCP currents were recorded. The vertical velocity shear was then calculated as:

$$\delta v = v\big(n_{up}(t)\big) - v\big(n_{lo}(t)\big) \qquad \text{(Eq. 2)}$$

Differently, n_{up} depends on many factors, including the tidal phase (which changes the position of the sea surface concerning the bottom) and the surface wave field (which affects the reflection of ADCP signals). To determine n_{up} the following methodology was used. For all possible integers n we computed the root mean square RMS for the velocity difference between two consecutive cells:

$$RMS_{\delta v_n} = \sqrt{< \big(v(n_\zeta - n + 1) - v(n_\zeta - n)\big)^2 >} \qquad \text{(Eq. 3)}$$

where n_ζ is the index of the cell whose centre is the closest to the air-sea interface in the water, and $<.>$ is the time-averaging operator over a M_2 tidal cycle (approximately 12.42 hours).

$RMS_{\delta v_n}$ was remarkably constant in the subsurface and suddenly jumped to a significantly larger value (by a factor of three or more) when approaching the surface. Although this discontinuity may partly be physical, it was used to define n_{up} above which ADCP data are considered possibly contaminated by side-lobe reflection and discarded. Corresponding n_{up} indices are $n_{\zeta} - 4$, $n_{\zeta} - 3$, and $n_{\zeta} - 2$ for the West, Centre, and East moorings, respectively (see **Fig. 2).** The western ADCP had a smaller bin size of 0.5 m, so the West and East moorings had their uppermost velocities at the same depth below the sea surface.

2.4.2. Larval densities related to location and tidal cycle

A series of two-sample t-tests assuming unequal variances was conducted to compare the densities (ind m^{-3}) of Clupeidae, Cynoglossidae, Gerreidae, and Mugilidae larvae under ebb and flood tide conditions at the West, Centre, and East locations. Ebb and flood conditions were determined using meridional velocity (ebb corresponds to the southward movement of water exiting the estuary; flood corresponds to the northward movement of water entering the estuary). Larval concentrations were transformed using ($Log_{10}(x+1)$) to meet the assumption of normality, and the goodness of fit was tested using the Shapiro–Wilk test (González-Estrada and Cosmes, 2019).

2.4.3. Vertical and length-frequency distribution of fish larvae

A two-way (factorial) analysis of variance (ANOVA) was conducted to compare the main effects of depth and tide and their interaction effect on larval transport at the different sampling locations. Larval transport (ind m^{-3} s^{-1}) was calculated by multiplying the current velocity (from the ADCP moored at the sampling location, in meters per second) by the larval density (number of larvae per m^3). The larval transport data were transformed using ($Log_{10}(x+1)$) to meet the assumption of normality, and goodness of fit was assessed using the Shapiro–Wilk test. The volume of the water column was not factored into this calculation. Since various transformations failed to normalize the data and stabilize the variance, a nonparametric Mann-Whitney test was conducted to investigate whether larval fish sizes differed between those entering the estuary (flood condition) and those leaving the estuary (ebb condition).

3. Results

3.1. Physical conditions during the high-resolution July measurements

Salinity temporal changes appeared similar at all three moorings, with salinity maxima coinciding with the reversal from ebb to flood (compare **Figs. 2** and **3**). This quadrature phase between velocity and salinity is consistent with the idea that the salinity field (increasing toward the head of the estuary, see **Fig. 4**) is repetitively moved past the moorings by the cyclic longitudinal barotropic flow. By integrating tidal flow over time, longitudinal ebb/flood tidal excursions of 10-12 km were obtained. These observations and the temporal change in salinity allow us to estimate the lateral salinity and density gradient in the estuary near the moorings, 0.25 psu km^{-1}.

Stratification varied greatly over the full observational period. Surface-to-bottom salinity differences (not shown) range from zero to three psu but are frequently 0.5, a typical value for the three moorings. Combining this number with the one for the lateral salinity gradient provided an estimate for the isohaline slope of 0.5 %, *e.g.*, quite similar to those found for the Shark Bay (Australia) inverse system (Hetzel et al., 2013).

Close inspection of the ADCP measurements (**Fig. 2**, lower panels) reveals the presence of positive vertical shear; near-surface waters exhibit more pronounced northward velocities, while near-bottom waters show more pronounced southward velocities. This is confirmed by the time series of velocity measured at the lowest and highest valid ADCP bins (**Fig. 2**, upper panels). Some spatio-temporal complexity is evident in the vertical shear (proportional to the separation distance between the red and blue curves) due to the variability of turbulence induced by bottom friction (which varies greatly over a tidal cycle but naturally favours positive shear during the flood), turbulence induced by air-sea interactions, and possibly pre-existing small-scale heterogeneities in stratification transported from outside the estuary by tidal flow.

The lack of measurements in the surface and bottom layers prevented us from presenting full water column transport budgets. Still, vertical shear averaged over one tidal cycle is robustly positive at the West and Centre ADCPs, with a mean velocity difference between near-surface and near-bottom waters of 0.09 m s^{-1} (West) and 0.05 m s^{-1} (Centre). These differences would presumably be even larger if velocities closer to the surface and bottom were available. At the East mooring, near-surface and near-bottom velocities differed most of the time, but their averages over a tidal cycle remain within 0.01 m s^{-1} of each other. Averaging over all three mooring locations and assuming a near-zero net flow across our measurement section, these numbers imply the existence of a mean southward flow with an intensity of approximately 0.025 m s^{-1} near the bottom depth and a northward flow of similar intensity near the surface. A slight volume imbalance is possible over a couple of tidal cycles, but additional arguments are provided in the discussion section to support the significance of the flow vertical shear and its importance for fish reproduction.

3.2. The Sine-Saloum thermohaline seasonal cycle

No current measurements are available for the sampling periods other than the one in July 2014. However, the nature of the estuarine circulation can be inferred from the analysis of vertical stratification (**Fig. 4a**) and longitudinal salinity gradient (**Fig. 4b**) as a function of the season. Longitudinal salinity differences between the bottom and surface are shown for two different sectors: the lower and middle estuary and the middle and upper estuary (see **Fig. 1** for locations). Vertical stratification higher than 0.5 psu was present at all locations in June, July, and August. In

November 2013, a similar magnitude of vertical stratification was only found in the downstream area.

Horizontal contrasts of salinity reveal a noticeable shift in the lower part of the Saloum from classical estuary conditions in November 2013 (Mid-Down salinity values < 0 at both surface and bottom) to inverse estuary conditions (Mid-Down salinity values > 0, albeit only slightly, in February 2014) (**Fig. 4b).** The time series of salinity contrasts in the upper Saloum differs in that no sign of reversal was seen between November 2013 and February 2014. More data points are needed to characterize the seasonal cycle accurately. Still, the robust signs of vertical stratification of the up-estuary salinity gradient and vertical stratification in **Fig. 4** are consistent with the dominance of "inverse estuary" conditions accompanied by gravitationally sheared flow.

3.3. Larval densities related to location and tidal cycle

Visual trends were evident for all taxa (Clupeidae, Cynoglossidae, Gerreidae, and Mugilidae), with higher densities during flood conditions in almost all cases. Two-sample t-tests were conducted for each family at each of the three sampling locations to test if these visual trends indicated statistical differences in larval densities between tidal conditions. Although visual differences in densities between ebb and flood conditions were observed for Clupeidae larvae at all three stations (Fig. 5a), these differences were not statistically significant (**Table 1**). Therefore, no effects of tidal conditions on Clupeidae larval densities could be detected statistically. Regarding Cynoglossidae larvae, no differences in larval densities were observed at the West and East stations, but a significant difference was found at the Centre location (t(5) = 3.60, p = 0.0156). This was expected because, at the Centre location, Cynoglossidae larvae were completely absent in the catches during ebb tide (Fig. 5b). Densities of Gerreidae larvae at the West and Centre locations were visually higher (Fig. 5c) between the tidal cycles (ebb *vs*. flood). Still, significant differences were only found at the East station (t(6) = 4.61, p = 0.0037), where Gerreidae larvae were absent in the catches during ebb tide (Fig. 5c). Lastly, the Mugilidae larval densities (Fig. 5d) differed significantly between tidal conditions at two locations, the Centre and East stations (Centre: t(7.6) = 3.73, p = 0.0064; East: t(10) = 2.28, p = 0.0455). No significant differences between ebb and flood densities were detected at the West location.

3.4. Larval transport related to location and time of day

Clupeidae larval transport showed a similar trend at all three sampling locations (**Fig. 6a**). Maximum relative transport (0.34 ind m^{-3} s^{-1}) occurred at the Centre, followed by the West (0.16 ind m^{-3} s^{-1}) and East (0.10 m^{-3} s^{-1}) locations. At all three locations, the highest transport numbers were obtained shortly after sunset, between 19:00 and 21:00 UTC. Cynoglossidae larval transport did not show a clear tendency to match between the locations (**Fig. 6b**), with maximum transport (0.03 m^{-3} s^{-1}) occurring at the East location shortly before sunset, between 16:00 and 18:00 UTC. Almost equally high transport (0.028 m^{-3} s^{-1}) occurred at the Centre location, but this time shortly after sunset, between 19:00 and 21:00 UTC. For Gerreidae larvae (**Fig. 6c**), the highest transport (0.13 m^{-3} s^{-1}) occurred at the East location, followed by the West location (0.03 m^{-3} s^{-1}) and the Centre location (0.01 m^{-3} s^{-1}). The highest transport at the East location occurred shortly before sunset, between 16:00 and 18:00 UTC, while the highest transport rates at the West and Centre locations occurred shortly after sunset, between 19:00 and 21:00 UTC. Mugilidae larval transport showed a similar trend between the West and Centre locations (**Fig. 6d**), with larval transport remaining low over most of the ~24-hour observation period. The highest density (0.21 m^{-3} s^{-1}) occurred at the East location, followed by the Centre (0.07 m^{-3} s^{-1}) and West (0.05 m^{-3} s^{-1}) locations. The highest densities were obtained at the East location shortly after sunset, between 19:00 and 21:00 UTC, at the Centre location shortly after sunrise, between 07:00 and 08:00 UTC, and at the West location in the middle of the day, around noon UTC. Overall, for the four taxa, a similar trend was observed. The highest larval transport occurred in a relatively short time window between 16:00 and 21:00 UTC, shortly before and after sunset. Additionally, Clupeidae exhibited the highest larval transport measurements at the Centre location, whereas Cynoglossidae, Gerreidae, and Mugilidae showed the highest measurements at the East location. Furthermore, larval transport for all families, except Clupeidae, increased shortly after sunrise.

3.5. Vertical distribution of fish larvae

3.5.1. Patterns and periodicity in pelagic larval vertical distribution

Larval transport fluctuations and changes in the vertical distribution of Clupeidae, Cynoglossidae, Gerreidae, and Mugilidae fish larvae over the ~24-hour sampling period are presented by time and tidal conditions (**Fig. 7**). None of the four taxa displayed apparent patterns of time- or tide-related vertical movement across the three strata of the water column that were sampled. Clupeidae and Cynoglossidae larvae consistently showed higher larval transport in the Mid-Water stratum at all locations, while Mugilidae larvae, and to a lesser extent Gerreidae larvae, consistently showed higher larval transport in the Surface stratum. For each of the four taxa, a two-way (factorial) analysis of variance was conducted to examine the influence of larval position in the water column and tide condition on larval transport at the three sampling locations (**Table 2**). Larval position in the water column, labelled "depth," included three levels (Surface, Near Surface, and Mid-Water), and the tide condition consisted of two levels (ebb and flood). Across taxa and locations, not all effects (Tukey post-hoc test) were significant (**Tables 2** and **3**). At all three locations, the larval position in the water column (depth) significantly affected Clupeidae's larval transport (West: $p = 0.0010$; Centre: $p = 0.0001$; East: $p = 0.0001$). A post-hoc Tukey test indicated that the mean larval transport score for the Mid-Water stratum was significantly higher than those for the Surface and Near Surface strata (**Table 3**). The same pattern was observed for Cynoglossidae larvae (West: p

= 0.0005; Centre: $p = 0.0020$; East: $p = 0.0005$), with the Mid-Water stratum having significantly higher mean larval transport scores than the Surface and Near Surface strata (**Table 3**). Gerreidae larval transport was more evenly distributed across all three water strata, with no significant effect of their position in the water column (depth) detected. Thus, there was no statistically detectable preference for any stratum. However, comparing the number of individuals sampled in each water stratum (Appendix B), Gerreidae larvae were consistently more abundant in the Surface stratum than in the Near Surface and Mid-Water strata, indicating a preference for the Surface stratum. Mugilidae larvae were almost exclusively located in the Surface stratum at the Centre and East locations (Centre: $p < 0.0001$; East: $p = 0.0291$). However, as larval transport at the West location was mostly null throughout the ~24-hour sampling period, no significant difference was detected at that location. Appendix B provides further evidence for the depth preferences of all four taxa.

3.5.2. Length-frequency distribution of fish larvae

The length-frequency distributions of Clupeidae, Cynoglossidae, Gerreidae, and Mugilidae larvae are presented by tide condition (ebb and flood), depth (Surface, Near Surface, and Mid-Water strata), and location (East, Centre, and West stations) (**Fig. 8**). In addition to the size distributions, the previously observed general patterns of vertical distribution showed that Clupeidae and Cynoglossidae larvae were predominantly found in the Mid-Water stratum, Gerreidae larvae were more evenly distributed across the three strata, and Mugilidae larvae mainly occurred in the Surface stratum. The length-frequency distributions for the four taxa of fish larvae, in terms of the size range observed, were quite homogeneous across the three strata and locations (**Fig. 8**). The differences in size distribution were minimal between samples categorized as ebb and flood conditions. Further, negligible differences in size distribution were apparent between locations and positions in the upper part of the water column. These findings present evidence of strong depth preferences independent of tidal conditions and location at the mouth of the Saloum branch of the Sine Saloum Estuary. Therefore, the species sampled showed no strong evidence of depth regulation based on tidal conditions or location. For all four taxa of fish larvae, larval size during the ebb tide was not significantly different from larval size during the flood tide (**Table 4**). This indicates that larvae entering and exiting the estuary are of a similar size range and not from distinctly.

4. Discussion

The use of estuarine nursery areas is a vital stage in the life cycle of many marine organisms, including several commercially important fish species (Boehlert and Mundy, 1988; Haedrich, 1983). In the Sine Saloum Estuary, Diouf (1996) highlighted the downstream section as particularly significant for reproductive activities, noting a high prevalence of fecund females and frequent spawning events. This observation is further supported by the high larval abundance recorded in the downstream sections (Sloterdijk et al., 2017) of this estuary. Generally, the presence of high larval densities in the downstream estuarine areas underscores the critical importance of connectivity between nearshore coastal and estuarine habitats, and previous studies have emphasized the role of larval transport mechanisms in fish recruitment and population sustainability. Our findings provide new insights into these dynamics within an inverse estuary environment. By integrating physical and biological observations, we identified gravitational circulation and the depth preferences of fish larvae as key drivers of larval transport in the Sine Saloum Estuary. Our observations suggest that, in contrast to the selective tidal stream transport (STST) typically seen in classical estuaries (*e.g.*, Melville-Smith et al., 1981; Holt et al., 1989; Joyeux, 1999, 2001; Chang et al., 2000; Teixeira Bonecker et al., 2009; Pattrick and Strydom, 2014; Lyczkowski-Shultz et al., 1990), the transport dynamics in this system are primarily influenced by gravitational circulation. This finding aligns with research by Roper (1986) in the Whangateau Harbour, New Zealand, which examined larval transport under comparable conditions.

Gravitational circulation, rather than STST, appears to be the primary driver of larval transport in the inverse Sine Saloum Estuary. For Clupeidae, Cynoglossidae, and Gerreidae, no dominant or clear patterns were observed in fish larval densities (**Table 1**) or larval transport relative to tidal conditions (**Table 2**). This suggests that, despite some apparent visual differences (*e.g.*, **Fig. 5**), the number of larvae exiting the estuary during the ebb tide was generally balanced by the number entering during the flood tide. Furthermore, no significant changes in the vertical position of the larvae were detected (**Fig. 7**). Regarding diurnal variations, a peak in abundance was observed in the hours preceding and shortly after sunset (**Fig. 6**). However, no additional data were available to determine whether this pattern would have persisted over time (*i.e.*, over multiple days and tidal cycles).

Concerning current and physico-chemical measurements, salinity changes at all three moorings followed a pattern with maxima coinciding with tidal reversal, indicating cyclic longitudinal barotropic flow. Stratification varied, with surface-to-bottom salinity differences typically around 0.5 psu and an isohaline slope of 0.5 %. Gravitational shear was evident (**Fig.2**), with near-surface waters showing more pronounced northward velocities and near-bottom waters exhibiting stronger southward velocities, confirming positive vertical shear. Velocity differences between near-surface and near-bottom waters averaged 0.09 m s^{-1} at the West mooring and 0.05 m s^{-1} at the Centre mooring, suggesting a mean southward flow near the bottom and northward flow near the surface. Based on the coupled observations of currents and larval distributions, the alternative we hypothesize for larval transport into or out of the estuary results from interactions between vertically sheared low-frequency currents (**Fig. 2**) present in the estuary (*i.e.*, ebb/flood tidal currents averaged out) and appropriate positioning of the larvae in the water column (**Fig. 7**). From a behavioural perspective, this mechanism can be viewed as simpler than STST in that it does not require the organisms to synchronize their vertical migrations with the phase of the tidal currents. First, the current characteristics provided circumstantial evidence for the existence of a longitudinal gravitational circulation in the Sine Saloum Estuary, as in other inverse estuaries (Nunes Vaz et al., 1990; Hetzel et al., 2013; Nidzieko and Monismith, 2013). This type of vertically sheared circulation could be of critical importance in the context of fish recruitment because it offers a natural path into (resp. out of) the estuarine system for organisms that would be able to maintain themselves in the upper (resp. lower) part of the water column. Second, the depth distribution of the fish larvae we presented exhibited two distinct patterns that varied depending on the taxon. Clupeidae and Cynoglossidae larvae were almost exclusively distributed in the Mid-Water stratum (**Fig. 7a & b**). Mugilidae larvae were exclusively distributed in the Surface and Near Surface water strata (**Fig. 7d**); likewise, although a bit more broadly distributed in the three water strata, Gerreidae larvae had all their peak densities and highest larval transport in the surface stratum (**Fig. 7c**). Again, we stress that no significant changes in vertical distribution of the four taxa of fish larvae with the tidal phase were noticeable (**Table 2**), which rules out that STST type strategies were important for larval transport at the time of the experiment.

On the other hand, maintenance into their preferred stratum plausibly led Clupeidae and Cynoglossidae (resp. Mugilidae) larvae to move toward the Saloum mouth and (resp. away from the Saloum mouth). The general transport tendency for Gerreidae larvae could not be determined with great confidence given uniform distribution. Still, peaks in abundance were systematically close to the surface, so their mean displacement may have been into the estuary. For all taxa, it is unclear, however, if the larvae actively maintained their position in the water column or if their specific buoyancy allows them to do so. If the latter were true, the proposed mechanism would be an efficient and low-cost way for fish larvae to move toward their nursery areas, requiring only the maintenance of position within a preferred depth range to utilize the prevailing flow patterns.

A caveat concerns the exact position of Clupeidae and Cynoglossidae larvae in the water column. Indeed, the lack of vertical resolution in larval sampling does not allow us to distinguish larvae in the water column away from the surface, where no weak gravitational flow is expected, from larvae adjacent to the bottom, where the strongest outflow resides. Another important limitation is that our current and larval sampling data are for the main Saloum entrance and cover ~ 2.5 tidal cycles during the end of the July warm/dry and low wind period. Caution is thus needed in their interpretation, but less comprehensive observations of salinity (**Fig. 4**) and temperature made during other field experiments (Sloterdijk et al., 2017) offer robust evidence that stratified conditions are prevalent in the estuary. Based on theoretical arguments and observations made in other inverse estuaries, we thus expect the vertically sheared gravitational circulation that permits the two-way larval transport between the estuary and the ocean to be a recurrent flow feature. Calm atmospheric conditions (as during our sampling period) and neap tides associated with weak oceanic turbulence favour the maintenance of some near-surface to-bottom stratification and are generally linked with the presence of vertically sheared gravitational currents in estuaries (Linden and Simpson, 1986; Hearn and Robson, 2002; Hetzel et al., 2015). The only exception was found during the cold season (in Feb. 2014) when fully mixed temperature and salinity vertical profiles were encountered so that the gravitational circulation may not have been present (**Fig. 4a**). Winter conditions when winds are strongest and heat fluxes most prone to intense vertical mixing are expected to stop the gravitational circulation, albeit perhaps intermittently depending on synoptic variability, *e.g.*, upwelling events or relaxations (Ndoye et al., 2014). For the marine species taking advantage of the inverse estuary gravitational circulation to achieve larval transport in or out of the Saloum, the cold/dry winter season would thus be the one presenting, on average, particularly unfavourable recruitment conditions to be avoided. In the Sine Saloum Estuary, Sloterdijk et al. (2017) observed that the seasonal abundance of the Clupeidae, Cynoglossidae, and Gerreidae larvae was lowest in February (winter season), which may be seen as indirect support in favour of this hypothesis. We note that winter reduction in larval abundance might also be due to other factors, such as low temperatures.

Moreover, the larval transport patterns inferred from their depth distributions align broadly with the reproductive biology and ecology of Clupeidae, Cynoglossidae, Gerreidae, and Mugilidae, as documented in various studies worldwide. For instance, several species of Clupeidae (such as *Ethmalosa fimbriata* and *Sardinella* sp.) and Cynoglossidae (such as *Cynoglossus senegalensis*) found in the Saloum were abundant in coastal waters outside the estuary and are known to enter estuaries to spawn. The larvae mature in these estuaries before being transported back to the coastal environment (Charles-Dominique and Albaret, 2003., Albaret, 1999; Blaber, 2000). In contrast, Mugilidae generally remain in rivers and coastal lagoons for most of their life cycle, migrating to the sea to spawn (Chang et al., 2000; Koutrakis, 2004; Trape et al., 2009; McDonough and Wenner, 2003; McDonough et al., 2003, 2005). After hatching and a brief growth period, their larvae and juveniles recruit into inshore coastal waters, primarily lagoons and estuaries, at sizes of 10–30 mm standard length (Blaber, 1997). Similarly, Gerreidae adult species typically inhabit coastal systems such as lagoons and estuaries bordered by mangroves. Still, they spawn at sea throughout the year, with larvae and juveniles entering estuaries until reaching maturity (Blaber, 2000).

The developmental stages at which fish are present in inlets and estuaries influence their ability to behaviourally modify their transport (Boehlert and Mundy, 1988). Our study also examined potential relationships between larval length-frequency distributions and the tidal phase or water stratum of sampling. No significant differences in the standard mean length of the four larval taxa were detected between ebb and flood conditions (**Table 4**). This suggests that, at least within the sampling period, larvae entering the Saloum branch on flood tide did not split into distinct size groups retained in the estuary versus those transported back on the ebb tide. Comparisons of length-frequency distributions between water strata were limited due to the strong depth preferences observed, leading to some taxa's absence or very low abundance in certain strata. Thus, no ontogenetic behaviour favouring estuarine ingress or egress was detected. This implies that the hypothesis of larval transport without tidal vertical migration applies across all sizes and developmental stages, as sensory and behavioural abilities may not be necessary, thus removing the size-dependency associated with size-dependent tidal vertical migration (Boehlert and Mundy, 1988).

Although our observations indicated clear patterns of larval transport and depth preferences, additional experiments are necessary to strengthen these findings and assess their broader applicability. Long-term monitoring across multiple seasons will help evaluate the variability of larval transport mechanisms under different environmental conditions. Higher-resolution vertical profiling of larval distributions could further clarify transport dynamics near the bottom layers. These approaches contribute to a better understanding of larval transport dynamics in inverse estuaries, ultimately informing management strategies for conserving and sustainably using estuarine fisheries and providing valuable information to model expected changes in tropical estuarine conditions due to climate change.

5. Conclusion

Gravitational circulation plays a fundamental role in driving larval transport within an inverse estuary where tidal dynamics have a relatively minor influence. The depth preferences of key larval taxa, including Clupeidae, Cynoglossidae, Mugilidae, and Gerreidae, demonstrate the importance of vertical positioning to utilize estuarine flow patterns for transport. This mechanism provides an efficient alternative to selective tidal stream transport (STST), aligning with the ecological and reproductive traits of the studied species. Seasonal variations in estuarine hydrodynamics highlight the sensitivity of gravitational circulation to environmental changes, particularly during the cold, dry winter season when increased vertical mixing occurs. Such seasonal disruptions likely impact recruitment success and point to the vulnerability of tropical estuarine ecosystems to climatic and anthropogenic pressures. Long-term, high-resolution monitoring of larval transport mechanisms is essential to understand these dynamics better and to inform sustainable management of estuarine fisheries. Addressing these knowledge gaps will be important in the face of increasing environmental variability and its implications for tropical estuarine ecosystems.

Acknowledgements

The authors would like to thank all colleagues of the LABEP-AO at the Institut Fondamental d'Afrique Noire (IFAN) of the Université Cheikh Anta Diop de Dakar and the Centre de recherche océanographique de Dakar Thiaroye (ISRA/CRODT) for their support in Senegal. We would like to recognize the field assistance of Dr. Philippe Estrade (IRD, Locean), Dr. Timothée Brochier (IRD, UMMISCO), and Dr. Oumar Sadio (IRD, Lemar). Also, the authors thank IRD Senegal for logistical support and assistance, including a shallow water research vessel (DIASSANGA) and his Senegalese crew, particularly Ansou Manné (IRD, Sénégal) and César Tendeng (re-IRD). Lastly, we thank Constanze von Waldthausen, Stefanie Bröhl, and Dorothee Dasbach (ZMT, Germany) for their technical assistance.

Funding

This work has been supported by the tripartite French-German-Sub Saharan Africa project (AWA) "Ecosystem Approach to the management of fisheries and the marine environment in West African waters" (funded by BMBF and IRD, Project No. 01DG12073B) and EU Preface project grant

603521 and was ended under Triatlas from the European Union’s Horizon 2020 research and innovation programme under grant agreement No 817578.

Author contribution

Drafting the manuscript: HS. Conception/design of the research: PB and HS. Collection of data: HS, XC. Data analysis/interpretation: HS, PB, XC. Intellectual contributions on text/revisions: IN, PB. Fund acquisition: PB and WE. Coordination: PB. Final approval of the manuscript: all authors.

REFERENCES

Albaret, J., 1999. Les peuplements des estuaires et lagunes, in: Lévêque, C., Paugy, D. (Eds.), Les Poissons Des Eaux Continentales Africaines : Diversité, Écologie, Utilisation Par l'homme. IRD, Paris, pp. 325–349.

Beck, M. W., Heck, K. L., Able, K. W., Childers, D. L., Eggleston, D. B., Gillanders, B. M., et al. (2001). The Identification, Conservation, and Management of Estuarine and Marine Nurseries for Fish and Invertebrates. *BioScience* 51, 633. doi: 10.1641/0006-3568(2001)051[0633:TICAMO]2.0.CO;2

Blaber, S.J.M., 1997. Fish and Fisheries of Tropical Estuaries. Chapman and Hall, London.

Blaber, S.J.M., 2000. Tropical Estuarine Fishes Ecology, Exploitation and Conservation. Blackwell Science, London.

Boehlert, G. W., and Mundy, B. C. (1988). Roles of Behavioral and Physical Factors in Larval and Juvenile Fish Recruitment to Estuarine Nursery Areas. *Am. Fish. Soc. Symp.* 3, 61–67.

Brehmer, P., Chi, T. Do, Laugier, T., Lalo, F., Fiandrino, A., and Mouillot, D. (2011a). Field investigations and multi-indicators for shallow water lagoon management: perspective for societal benefit. *Aquatic Conservation: Marine and Freshwater Ecosystems* 21, 728–742.

Brehmer, P., Chi, T. D., and Mouillot, D. (2006). Amphidromous fish school migration revealed by combining fixed sonar monitoring (horizontal beaming) with fishing data. *Journal of Experimental Marine Biology and Ecology* 334, 139–150. doi: 10.1016/j.jembe.2006.01.017

Brehmer, P., Guillard, J., Pinzon, P. I. C., and Bach, P. (2011b). Exploratory and Instantaneous Swimming Speeds of Amphidromous Fish School in Shallow-Water Coastal Lagoon Channels. *Estuaries and Coasts* 34, 739–744. doi: 10.1007/s12237-011-9409-3

Chang, C. W., Tzeng, W. N., and Lee, Y. C. (2000). Recruitment and hatching dates of grey mullet (Mugil cephalus L.) juveniles in the Tanshui estuary of northwest Taiwan. *Zoological Studies* 39, 99–106.

Charles-Dominique, E., and Albaret, J.-J. (2003). African shads, with emphasis on the West African shad *Ethmalosa fimbriata*. *In* : American Fisheries Society Symposium. American Fisheries Society. p. 27-48

Churchill, Forward, Luettich, Hench, Hettler, Crowder, et al. (1999). Circulation and larval fish transport within a tidally dominated estuary. *Fisheries Oceanography* 8, 173–189. doi: 10.1046/j.1365-2419.1999.00025.x

De Silva, S. S., and Silva, E. I. L. (1979). Biology of young grey mullet, *Mugil cephalus* L., populatioins in a coastal lagoon in Sri Lanka. *Journal of Fish Biology* 15, 9–20. doi: 10.1111/j.1095-8649.1979.tb03568.x

Diouf, P.D., 1996. Les peuplements de poissons des milieux estuariens de l'Afrique de l'Ouest: L'exemple de l'estuaire hyperhalin du Sine-Saloum. PhD Thesis, UCDA, Dakar.

Forward Jr, Reinsel, Peters, Tankersley, Churchill, Crowder, et al. (1999). Transport of fish larvae through a tidal inlet. *Fisheries Oceanography* 8, 153–172. doi: 10.1046/j.1365-2419.1999.00026.x

Fukuda, N., Aoyama, J., Yokouchi, K., and Tsukamoto, K. (2016). Periodicities of inshore migration and selective tidal stream transport of glass eels, Anguilla japonica, in Hamana Lake, Japan. *Environmental Biology of Fishes* 99, 309–323. doi: 10.1007/s10641-016-0475-z

González-Estrada, E., and Cosmes, W. (2019). Shapiro–Wilk test for skew normal distributions based on data transformations. *Journal of Statistical Computation and Simulation* 89, 3258–3272. doi: 10.1080/00949655.2019.1658763

Haedrich, R.L., 1983. Estuarine Fishes, in: Ketchum, B.H. (Ed.), Estuaries and Enclosed Seas. Elsevier, Amsterdam, pp. 183–207.

Hearn, C. J., and Robson, B. J. (2002). On the effects of wind and tides on the hydrodynamics of a shallow Mediterranean estuary. *Continental Shelf Research* 22, 2655–2672. doi: 10.1016/S0278-4343(02)00119-X

Hetzel, Y., Pattiaratchi, C., and Lowe, R. (2013). Intermittent dense water outflows under variable tidal forcing in Shark Bay, Western Australia. *Continental Shelf Research* 66, 36–48. doi: 10.1016/j.csr.2013.06.015

Hetzel, Y., Pattiaratchi, C., Lowe, R., and Hofmeister, R. (2015). Wind and tidal mixing controls on stratification and dense water outflows in a large hypersaline bay. *JGR Oceans* 120, 6034–6056. doi: 10.1002/2015JC010733

Hjort, J. (1914). Fluctuations in the great fisheries of northern Europe viewed in the light of biological research. *Rapp. P.-V. Reun. Cons. Int. Explo. Mer* 20, 1–228.

Hjort, J. (1926). Fluctuations in the year classes of important food fishes. *ICES Journal of Marine Science* 1, 5–38. doi: 10.1093/icesjms/1.1.5

Holt, S. A., Holt, J., and Arnorld, C. R. (1989). Tidal streamtransport of larval fishes into non-stratified estuaries. *Rapp. P.-V. Reun. Cons. Int. Explo. Mer*, 100–104.

Joyeux, J.-C. (1999). The Abundance of Fish Larvae in Estuaries: Within-Tide Variability at Inlet and Immigration. *Estuaries* 22, 889. doi: 10.2307/1353069

Joyeux, J.-C. (2001). The retention of fish larvae in estuaries: among-tide variability at Beaufort Inlet, North Carolina, USA. *Journal of the Marine Biological Association of the United Kingdom* 81, 857–868. doi: 10.1017/S0025315401004696

Koutrakis, E. T. (2004). Temporal occurrence and size distribution of grey mullet juveniles (Pisces, Mugilidae) in the estuarine systems of the Strymonikos Gulf (Greece). *Journal of Applied Ichthyology* 20, 76–78. doi: 10.1111/j.1439-0426.2004.00501.x

Largier, J. L., Hollibaugh, J. T., and Smith, S. V. (1997). Seasonally Hypersaline Estuaries in Mediterranean-climate Regions. *Estuarine, Coastal and Shelf Science* 45, 789–797. doi: 10.1006/ecss.1997.0279

Lavín, M. F., Godínez, V. M., and Alvarez, L. G. (1998). Inverse-estuarine Features of the Upper Gulf of California. *Estuarine, Coastal and Shelf Science* 47, 769–795. doi: 10.1006/ecss.1998.0387

Leis, J.M., Carson-Ewart, B.M. (Eds.), 2004. The larvae of Indo-Pacific coastal fishes: An identification guide to marine fish larvae, Second edi. ed. Leiden, Boston.

Linden, P. F., and Simpson, J. E. (1986). Gravity-driven flows in a turbulent fluid. *Journal of Fluid Mechanics* 172, 481. doi: 10.1017/S0022112086001829

Lyczkowski-Shultz, J., Ruple, D. L., Richardson, S. L., and Cowan, J. H. (1990). Distribution of Fish Larvae Relative to Time and Tide in a Gulf of Mexico Barrier Island Pass. *Bulletin of Marine Science* 46(3), 563-577.

Mbow, C., Mertz, O., Diouf, A., Rasmussen, K., and Reenberg, A. (2008). The history of environmental change and adaptation in eastern Saloum–Senegal—Driving forces and perceptions. *Global and Planetary Change* 64, 210–221. doi: 10.1016/j.gloplacha.2008.09.008

McCleave, J. D., and Kleckner, R. C. (1982). Selective tidal stream transport in the estuarine migration of glass eels of the American eel (*Anguilla rostrata*). *ICES Journal of Marine Science* 40, 262–271. doi: 10.1093/icesjms/40.3.262

McDonough, C.J., Roumillat, W.A., Wenner, C.A., 2005. Sexual differentiation and gonad development in striped mullet (Mugil cephalus L.) from South Carolina estuaries. *Fishery Bulletin* 103, 601–619.

McDonough, C.J., Roumillat, W.A., Wenner, C.A., 2003. Fecundity and spawning season of striped mullet (Mugil cephalus L.) in South Carolina estuaries. *Fishery Bulletin* 101, 822–834.

McDonough, C.J., Wenner, C.A., 2003. Growth, recruitment, and abundance of juvenile striped mullet (Mugil cephalus) in South Carolina estuaries. *Fishery Bulletin* 101, 343–357.

Melville-Smith, R., Baird, D., and Woolridge, T. (1981). The utilization of tidal currents by the larvae of an estuarine fish. *South African Journal of Zoology* 16, 10–13. doi: 10.1080/02541858.1981.11447727

Miller, B. S., and Kendall, J. R. (2009). *Earl Life History of Marine Fishes*. Berkeley and Los Angeles: University of California Press.

Ndoye, S., Capet, X., Estrade, P., Sow, B., Dagorne, D., Lazar, A., Gaye, A., and Brehmer, P., (2014). SST patterns and dynamics of the southern Senegal-Gambia upwelling center. *Journal of Geophysical Research* 119, 8315-8335. doi:10.1002/2014JC010242.

Nidzieko, N. J., and Monismith, S. G. (2013). Contrasting Seasonal and Fortnightly Variations in the Circulation of a Seasonally Inverse Estuary, Elkhorn Slough, California. *Estuaries and Coasts* 36, 1–17. doi: 10.1007/s12237-012-9548-1

Norcross, B. L., and Shaw, R. F. (1984). Oceanic and Estuarine Transport of Fish Eggs and Larvae: A Review. *Transactions of the American Fisheries Society* 113, 153–165. doi: 10.1577/1548-8659(1984)113<153:OAETOF>2.0.CO;2

Nunes Vaz, R. A., Lennon, G. W., and Bowers, D. G. (1990). Physical behaviour of a large, negative or inverse estuary. *Continental Shelf Research* 10, 277–304. doi: 10.1016/0278-4343(90)90023-F

Pattrick, P., and Strydom, N. (2014). Recruitment of fish larvae and juveniles into two estuarine nursery areas with evidence of ebb tide use. *Estuarine, Coastal and Shelf Science* 149, 120–132. doi: 10.1016/j.ecss.2014.08.003

Pattrick, P., and Strydom, N. A. (2009). Swimming abilities of wild-caught, late-stage larvae of Diplodus capensis and Sarpa salpa (Pisces: Sparidae) from temperate South Africa. *Estuarine, Coastal and Shelf Science* 85, 547–554. doi: 10.1016/j.ecss.2009.09.022

Pineda, J., A. Hare, J., and Sponaugle, S. (2007). Larval Transport and Dispersal in the Coastal Ocean and Consequences for Population Connectivity. *Oceanography* 20, 22–39.

Roper, D. S. (1986). Occurrence and recruitment of fish larvae in a northern New Zealand estuary. *Estuarine, Coastal and Shelf Science* 22, 705–717. doi: 10.1016/0272-7714(86)90094-6

Simier, M., Blanc, L., Aliaume, C., Diouf, P. S., and Albaret, J. J. (2004). Spatial and temporal structure of fish assemblages in an "inverse estuary", the Sine Saloum system (Senegal). *Estuarine, Coastal and Shelf Science* 59, 69–86. doi: 10.1016/j.ecss.2003.08.002

Sloterdijk, H., Brehmer, P., Sadio, O., Müller, H., Döring, J., and Ekau, W. (2017). Composition and structure of the larval fish community related to environmental parameters in a tropical estuary impacted by climate change. *Estuarine, Coastal and Shelf Science* 197, 10–26. doi: 10.1016/j.ecss.2017.08.003

Tanaka, M., Goto, T., Tomiyama, M., and Sudo, H. (1989). Immigration, settlement and mortality of flounder (*Paralichthys olivaceus*) larvae and juveniles in a nursery ground, Shijiki Bay, Japan. *Netherlands Journal of Sea Research* 24, 57–67. doi: 10.1016/0077-7579(89)90170-1

Teixeira Bonecker, F., de Castro, M. S., and Teixeira Bonecker, A. C. (2009). Larval fish assemblage in a tropical estuary in relation to tidal cycles, day/night and seasonal variations. *Pan-American Journal of Aquatic Sciences* 4, 239–246.

Teodósio, M. A., Paris, C. B., Wolanski, E., and Morais, P. (2016). Biophysical processes leading to the ingress of temperate fish larvae into estuarine nursery areas: A review. *Estuarine, Coastal and Shelf Science* 183, 187–202. doi: 10.1016/j.ecss.2016.10.022

Thiaw, M., Gascuel, D., Sadio, O., Ndour, I., Diadhiou, H. D., Kantoussan, J., et al. (2021). Efficiency of two contrasted marine protected areas (MPA) in West Africa over a decade of fishing closure. *Ocean & Coastal Management* 210, 105655. doi: 10.1016/j.ocecoaman.2021.105655

Trape, S., Durand, J.-D., Guilhaumon, F., Vigliola, L., and Panfili, J. (2009). Recruitment patterns of young-of-the-year mugilid fishes in a West African estuary impacted by climate change. *Estuarine, Coastal and Shelf Science* 85, 357–367. doi: 10.1016/j.ecss.2009.08.018

Weinstein, M. P., Weiss, S. L., and Hodson, R. G. (1980). Retention of three taxa of postlarval fishes in an intensively flushed tidal estuary, Cape Fear River, North Carolina. *Fisheries Bulletin US* 78, 419-436.

Xenopoulos, M. A., Lodge, D. M., Alcamo, J., Märker, M., Schulze, K., and Van Vuuren, D. P. (2005). Scenarios of freshwater fish extinctions from climate change and water withdrawal. *Global Change Biology* 11, 1557–1564. doi: 10.1111/j.1365-2486.2005.001008.x

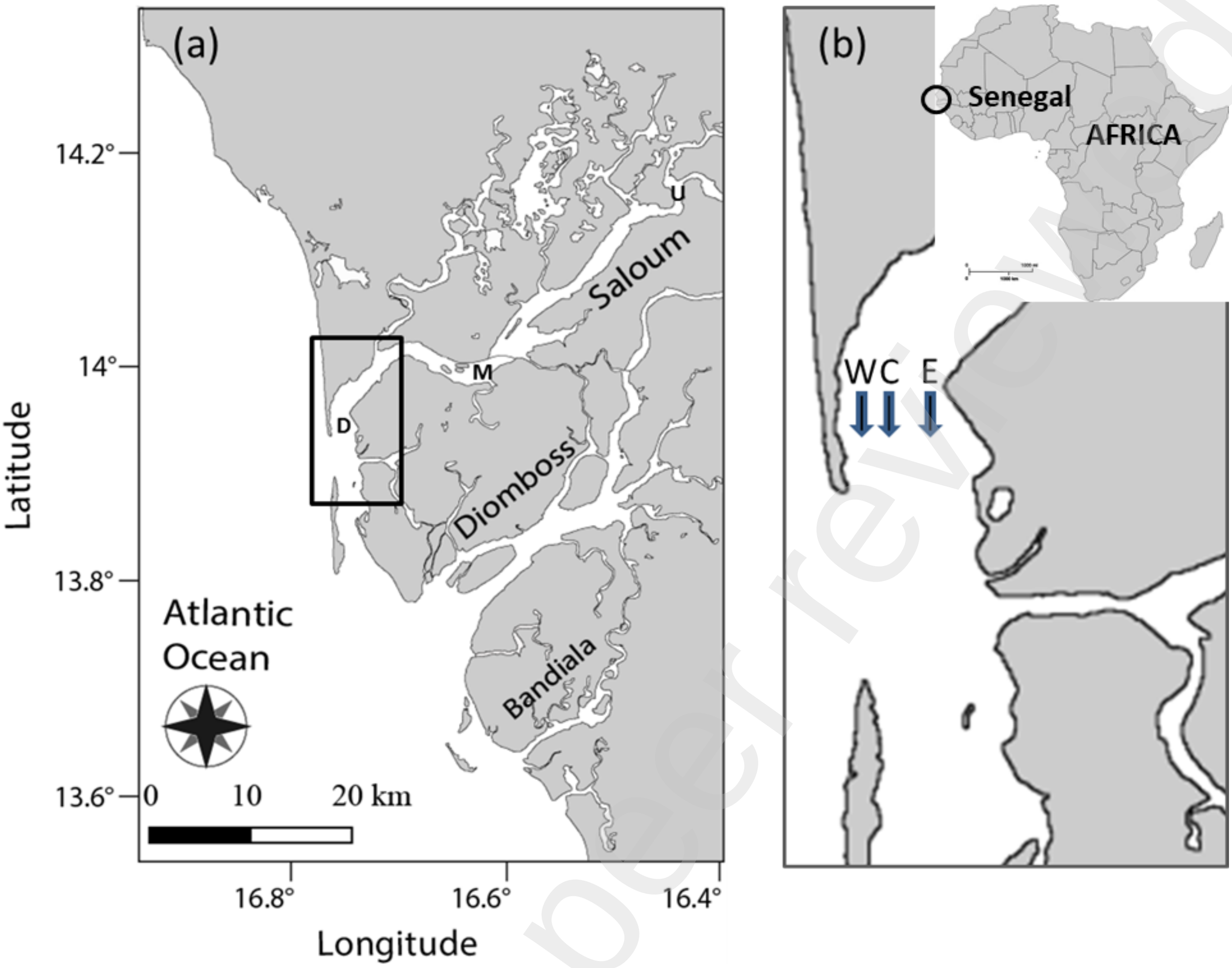

Fig. 1. (a) Location of the study system and the three sectors (D: Downstream, M: Midstream, U: Upstream). (b) Zoom showing the positions of the three sampling locations (W: West, C: Centre, E: East) at the mouth of the Saloum branch of the Sine Saloum Estuary (Senegal, West Africa).

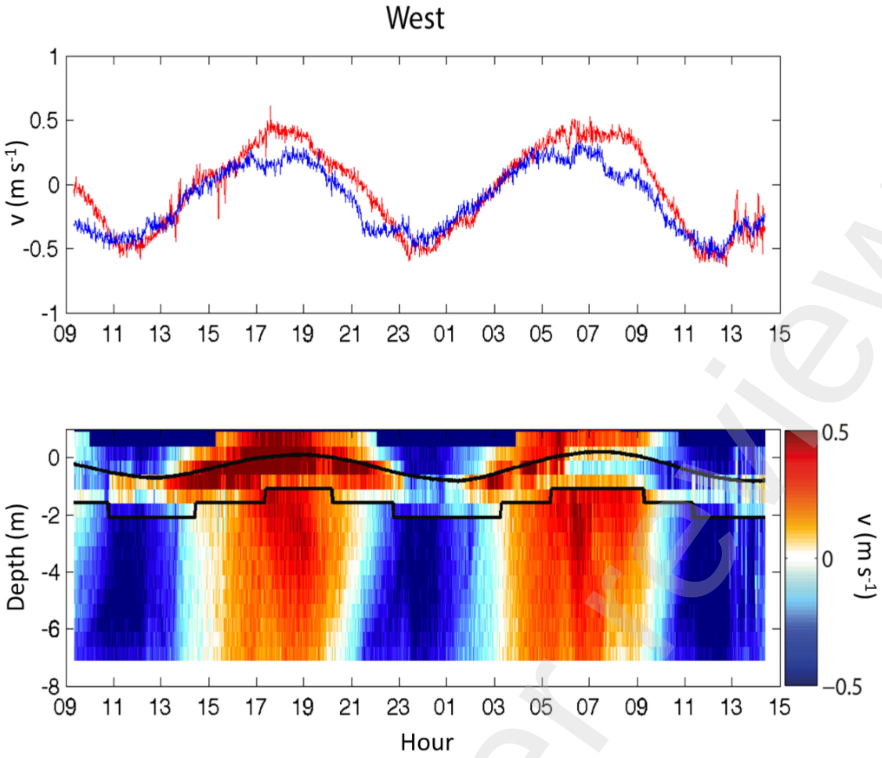
West
v (m s-1)
1
0.5
0
-0.5
-1
09
11
13
15
17
19
21
23
01
03
05
07
09
11
13
15
Depth (m)
0
-2
-4
-6
-8
0.5
0
−0.5
v (m s-1)
Hour

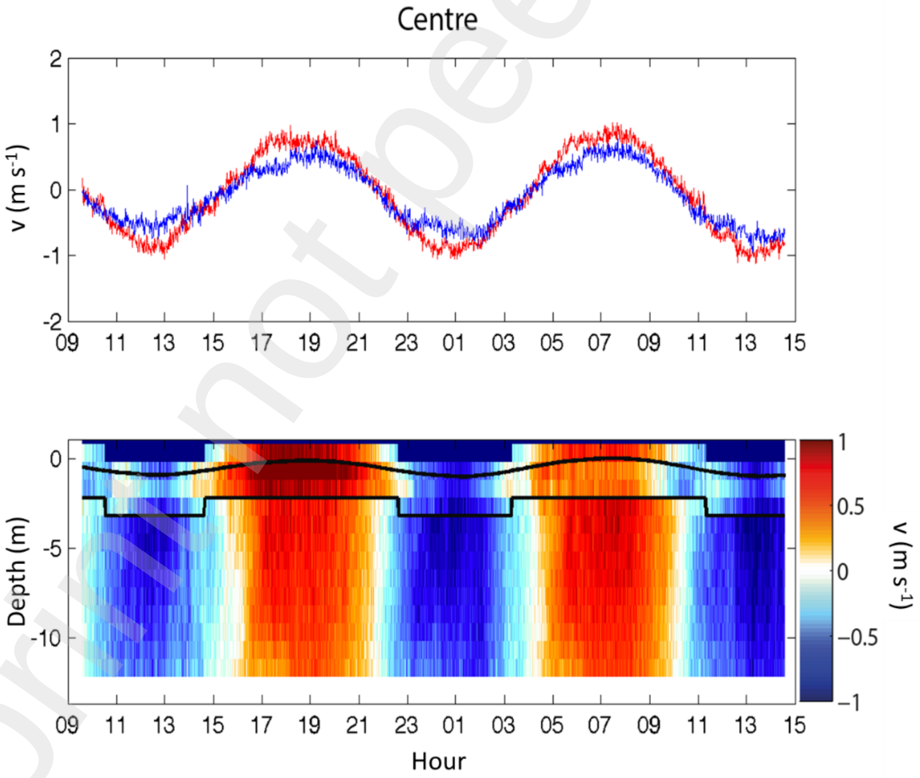
Centre
v (m s-1)
2
1
0
-1
-2
09
11
13
15
17
19
21
23
01
03
05
07
09
11
13
15
Depth (m)
0
-5
-10
1
0.5
0
−0.5
−1
v (m s-1)
Hour

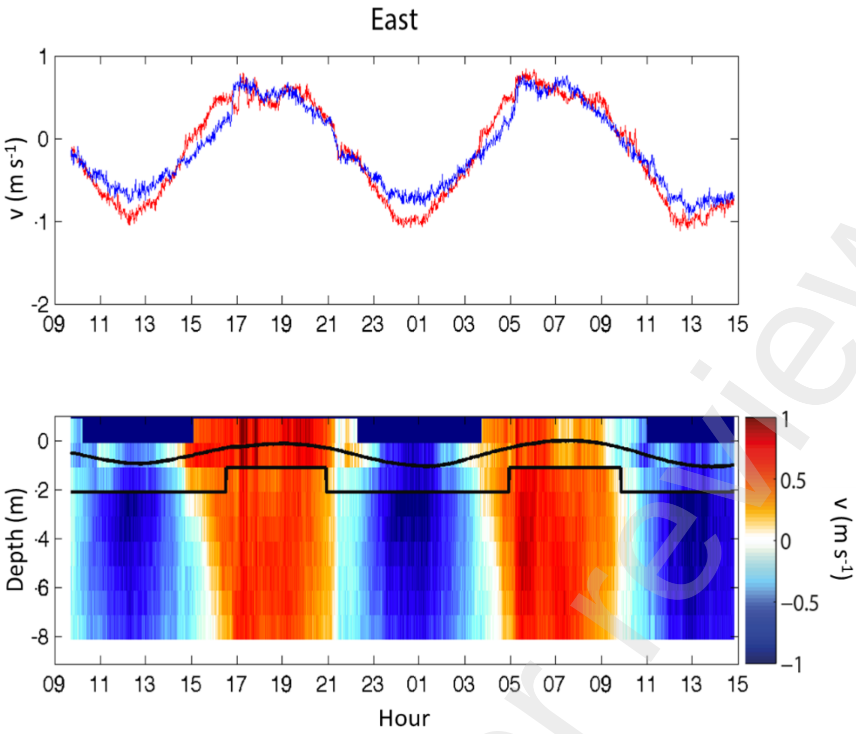

Fig. 2. Meridional velocity [m s^{-1}] measured from ADCPs at the western (upper), centre (middle), and eastern (lower) mooring locations in the Sine Saloum stations. The upper panels show the uppermost (red curve) and deepest (blue curve) valid velocities' time series. Complete depth-time diagrams for the entire deployment period are shown in the lower panels (in colour). The undulating black line represents the position of the air-sea interface. The step-like black line is situated at the top of the ADCP cell, which is used to compute near-surface to near-bottom velocity shear. This uppermost valid cell is the shallowest one situated at least 2 m (ADCP: West, 1000 kHz, and East, 600 kHz) or 3 m (ADCP: Centre, 400 kHz) below the free surface. Unit in [m s^{-1}] for the colour bar legend of the lower panels.

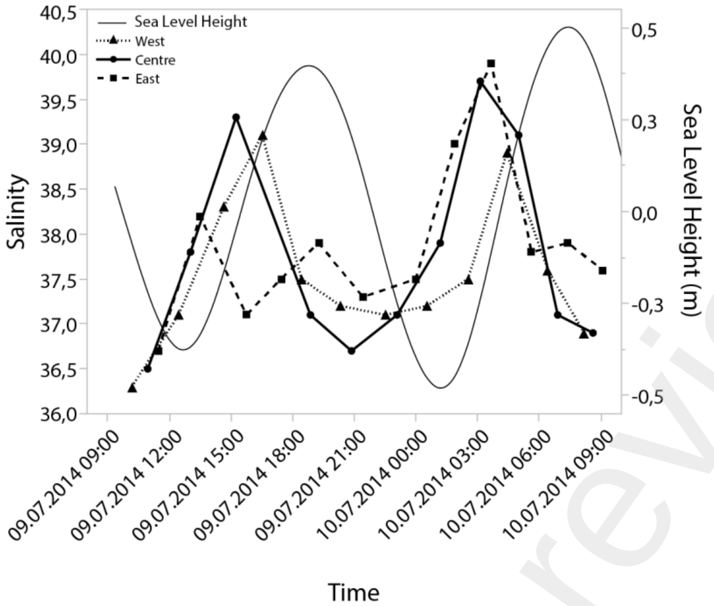

Fig. 3. Salinity variation and sea level height at the three stations at the head of the Saloum branch of the Sine Saloum Estuary. An approximate quadrature phase is observed between estuarine water salinity and velocities, *i.e.*, salinity maxima are obtained around 03 PM and 03 AM at the end of the ebb phase when waters reaching the moorings area are the ones that have the most estuarine characteristics possible (for a given tidal coefficient and excursion magnitude). Times are Coordinated Universal Time (UTC).

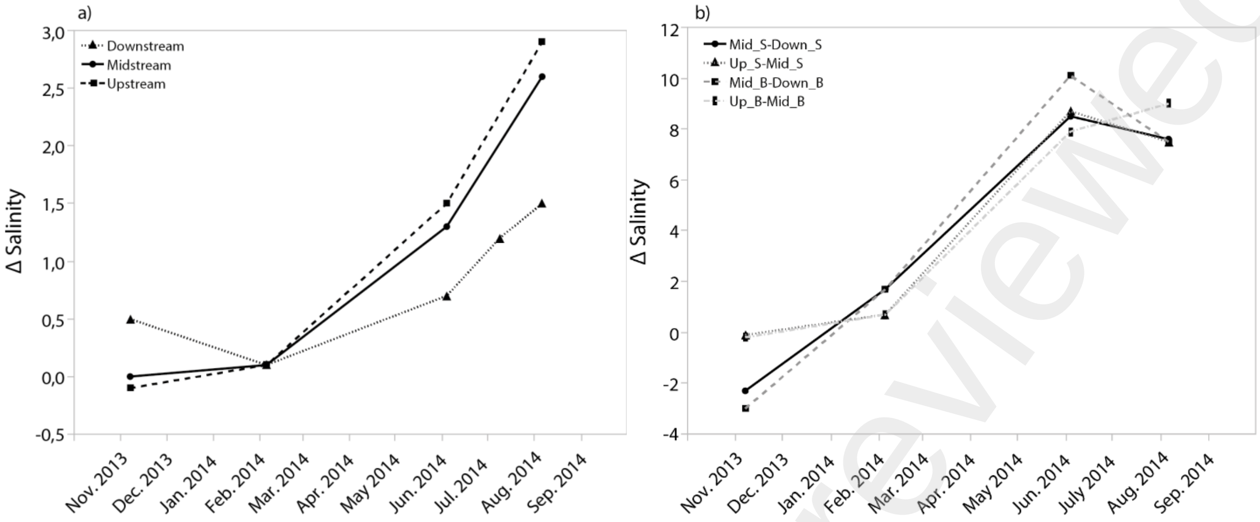

Fig. 4. Seasonal cycle (November 2013 to August 2014) for the (a) surface-to-bottom water column stratification due to salinity effects over the three different subareas referred to as downstream (Down), midstream (Mid), and upstream (Up) (see Fig. 1). (b) Lateral surface (S) and bottom (B) salinity contrast between the Midstream and Downstream, or Upstream and Midstream.

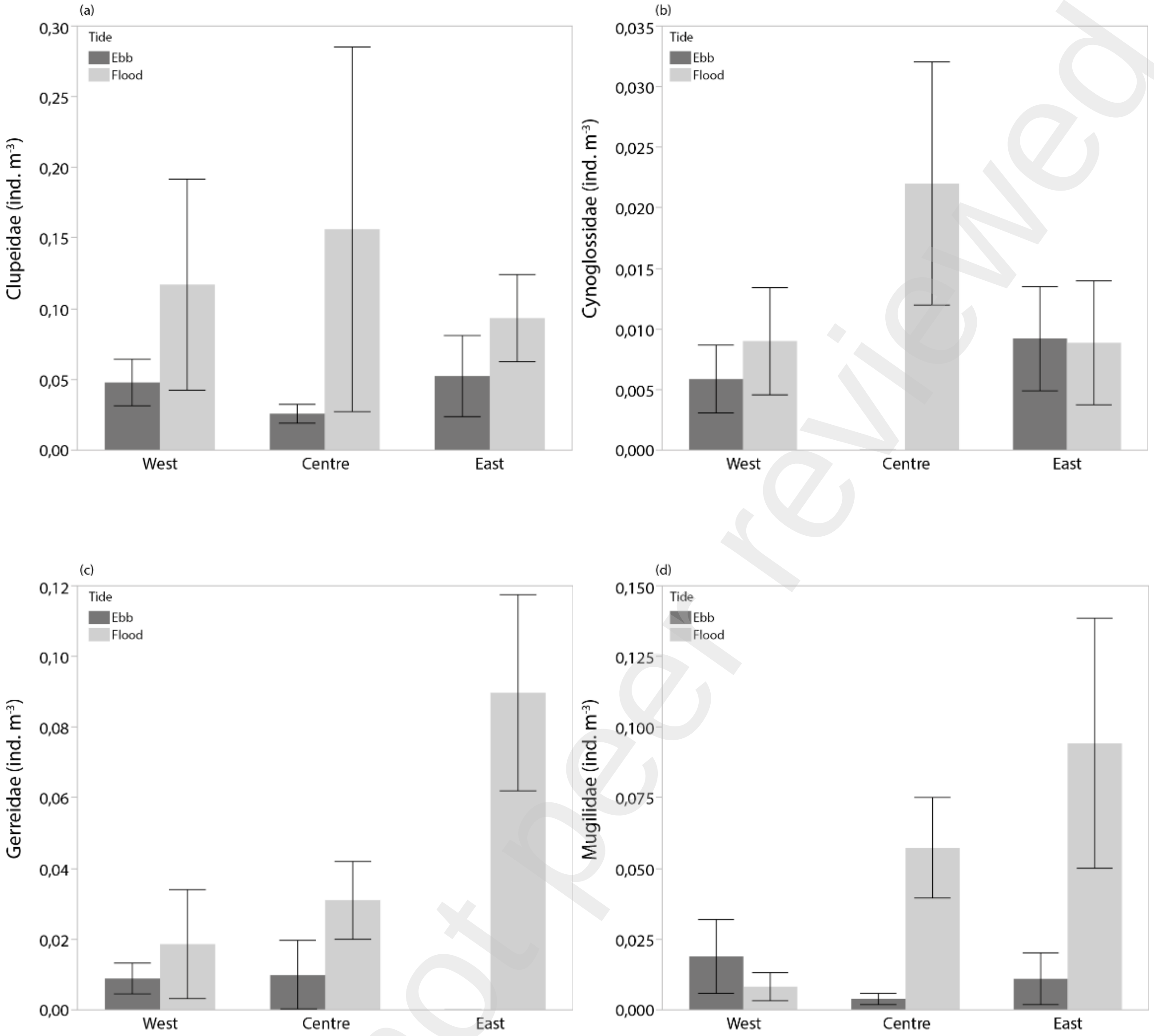

Fig. 5. Fish larvae densities (ind m^{-3}) of (a) Clupeidae, (b) Cynoglossidae, (c) Gerreidae, and (d) Mugilidae collected during ebb and flood tides at the West, Centre, and East stations located at the mouth of the Saloum branch of the Sine Saloum Estuary. Each error bar is constructed using one standard error from the mean.

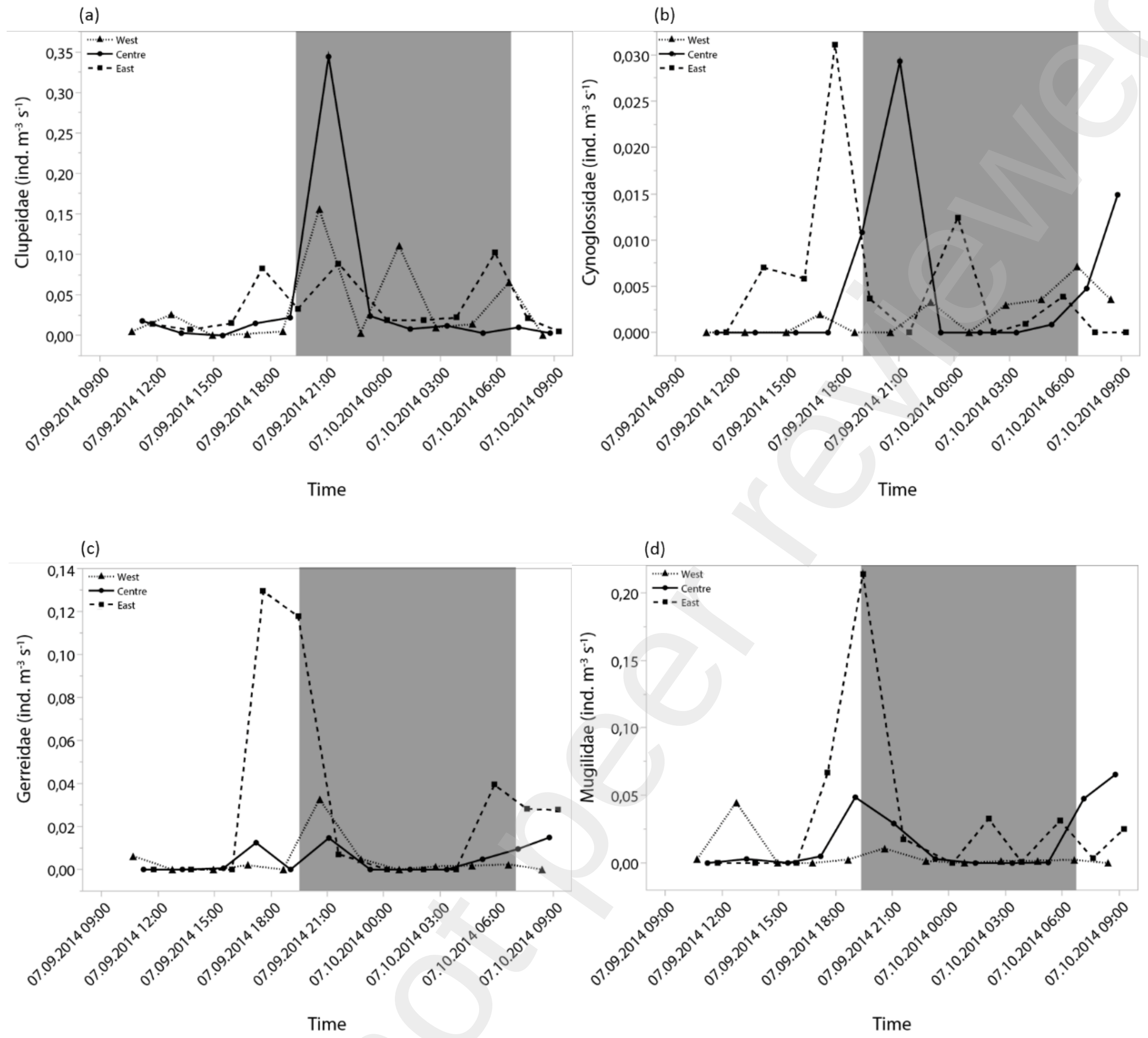

Fig. 6. Larval transport (ind m^{-3} s^{-1}) of Clupeidae, Cynoglossidae, Gerreidae, and Mugilidae collected on a two-hour time interval frequency over the ~24-hour sampling period at the West, Centre, and East locations with night-time periods shaded. Times are Coordinated Universal Time (UTC).

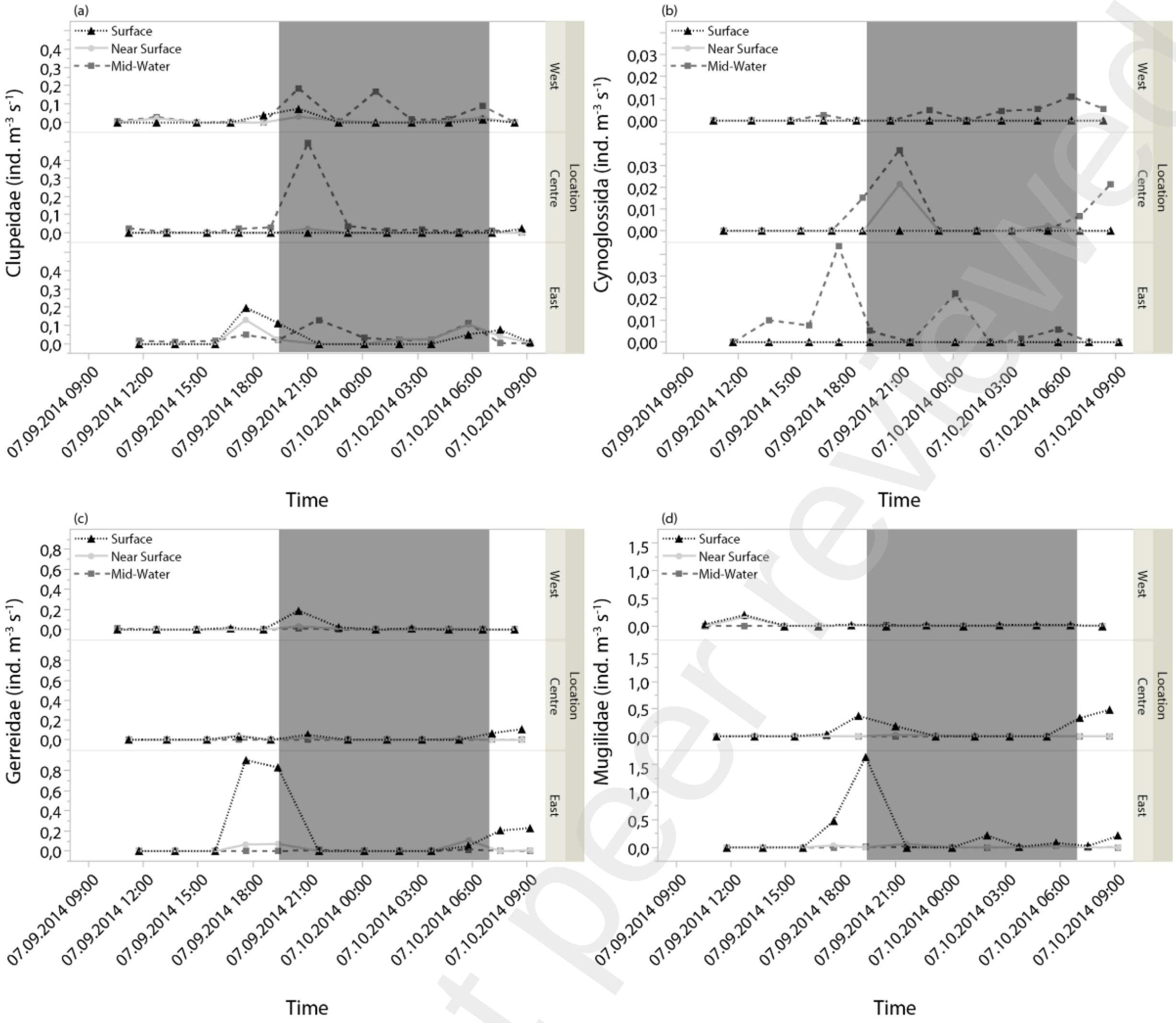

Fig. 7. Fish larvae densities (ind m^{-3} s^{-1}) of Clupeidae, Cynoglossidae, Gerreidae, and Mugilidae collected on a two-hour time interval frequency over the ~ 24 h sampling period at the West, Centre, and East stations in the Sine Saloum Estuary, and for the three vertical sampling position in the water column. Night-time periods are shaded, and times are Coordinated Universal Time (UTC).

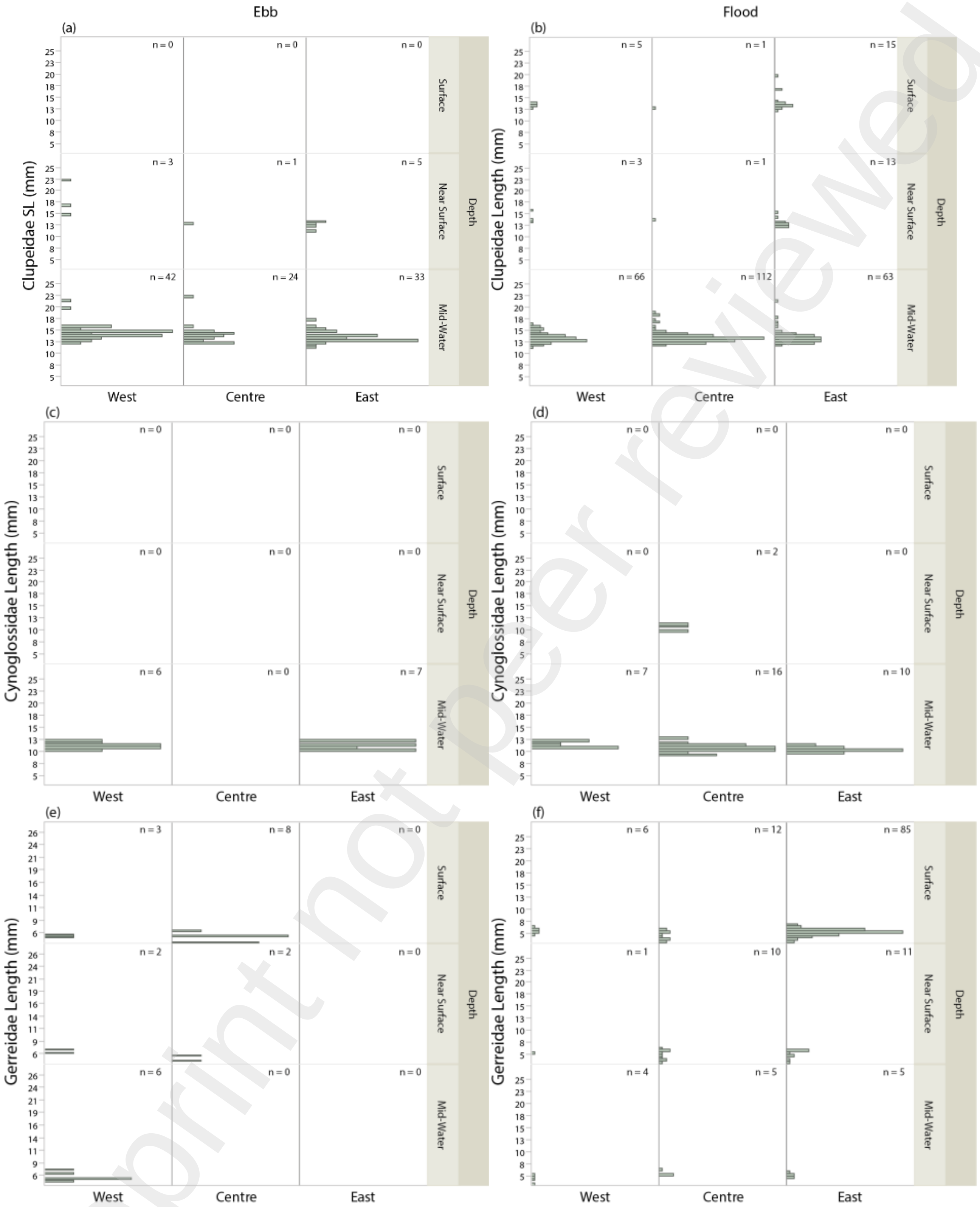
Ebb
Flood
(a)
(b)
(c)
(d)
(e)
(f)
Clupeidae SL (mm)
Clupeidae Length (mm)
Cynoglossidae Length (mm)
Gerreidae Length (mm)
Surface
Near Surface
Mid-Water
Depth
West
Centre
East
n = 0
n = 0
n = 0
n = 3
n = 1
n = 5
n = 42
n = 24
n = 33
n = 5
n = 1
n = 15
n = 3
n = 1
n = 13
n = 66
n = 112
n = 63
n = 0
n = 0
n = 0
n = 0
n = 0
n = 0
n = 6
n = 0
n = 7
n = 0
n = 0
n = 0
n = 0
n = 2
n = 0
n = 7
n = 16
n = 10
n = 3
n = 8
n = 0
n = 2
n = 2
n = 0
n = 6
n = 0
n = 0
n = 6
n = 12
n = 85
n = 1
n = 10
n = 11
n = 4
n = 5
n = 5
5
8
10
13
15
18
20
23
25
6
9
11
14
16
19
21
24
26

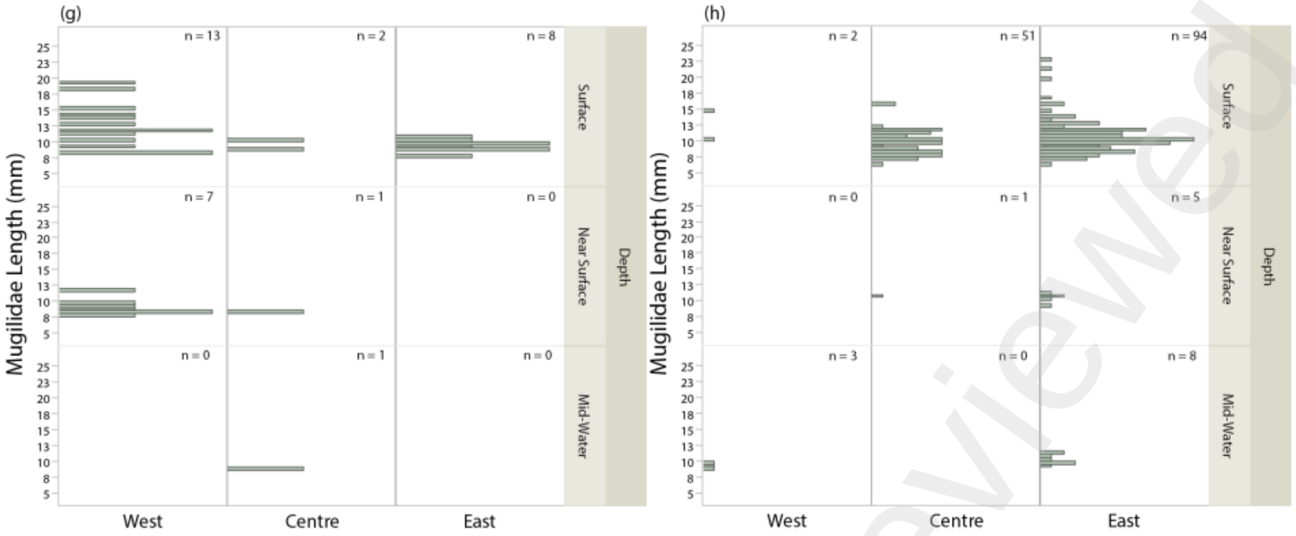

Fig. 8. Fish larvae length-frequency distribution of Clupeidae, Cynoglossidae, Gerreidae, and Mugilidae in three depth strata (Surface, Near Surface and Mid-Water) showing differences between ebb and flood tides samples in the Sine Saloum Estuary. Length corresponds to standard length (*i.e.*, measured from the tip of the snout to the end of the notochord, in mm).

Table

Larval Fish Transport Dynamics in an arid Estuary do not follow Selective Tidal Stream Transport Mechanisms

Hans Sloterdijk et al.

Table 1

Summary of the two-sample t-tests for fish larvae densities of Clupeidae, Cynoglossidae, Gerreidae, and Mugilidae by tidal conditions at the three locations of the estuary (West, Centre, East). Capital letters indicate significant differences, with "A" greater than "B". Non-significant is denoted with ns. Mean expressed as ind m^{-3}. SD = Standard deviation. * Show significant test at *p*-value < 0.05.

	Taxa	Ebb Mean (SD)	Flood Mean (SD)	Ebb	Flood	t value	p-value
West							
	Clupeidae	0.753 (0.398)	0.777 (0.732)	ns	ns	0.07	0.9496
	Cynoglossidae	0.204 (0.255)	0.301 (0.301)	ns	ns	0.58	0.5763
	Gerreidae	0.293 (0.331)	0.320 (0.409)	ns	ns	0.12	0.9039
	Mugilidae	0.383 (0.406)	0.241 (0.252)	ns	ns	-0.75	0.4726
Centre							
	Clupeidae	0.665 (0.236)	0.867 (0.589)	ns	ns	0.78	0.4616
	Cynoglossidae	0 (0)	0.498 (0.339)	B	A	3.60	0.0156*
	Gerreidae	0.174 (0.425)	0.635 (0.366)	ns	ns	2.02	0.0721
	Mugilidae	0.180 (0.207)	0.856 (0.393)	B	A	3.73	0.0064*
East							
	Clupeidae	0.828 (0.305)	1.057 (0.303)	ns	ns	1.29	0.2316
	Cynoglossidae	0.295 (0.304)	0.275 (0.315)	ns	ns	-0.11	0.9121
	Gerreidae	0 (0)	0.972 (0.558)	B	A	4.61	0.0037*
	Mugilidae	0.241 (0.392)	0.902 (0.608)	B	A	2.28	0.0455*

Table 2

Larval transport summary results from the two-way (factorial) analysis of variance and post-hoc connecting letter report for the four taxa of fish larvae collected at the surface, near-surface, and mid-water at the head of the Saloum branch of the Sine Saloum Estuary. Non-significant results are abbreviated "ns"(above *p*-value = 0.05), and capital letters indicate significant differences, with "A" being greater than "B".

	Taxa	Depth (D) *p*-value	Surface	Near-Surface	Mid-Water	Tide (T) *p* value	Ebb	Flood	*D x T* *p*-value
West									
	Clupeidae	0.0010	B	B	A	ns	ns	ns	ns
	Cynoglossidae	0.0005	B	B	A	ns	ns	ns	ns
	Gerreidae	ns	ns	ns	ns	ns	ns	ns	ns
	Mugilidae	ns	ns	ns	ns	ns	ns	ns	ns
Centre									
	Clupeidae	0.0001	B	B	A	ns	ns	ns	ns
	Cynoglossidae	0.0020	B	AB	A	0.0008	B	A	0.0020
	Gerreidae	ns	ns	ns	ns	0.0299	B	A	ns
	Mugilidae	0.0001	A	B	B	0.0011	B	A	0.0001
East									
	Clupeidae	ns	ns	ns	ns	ns	ns	ns	ns
	Cynoglossidae	0.0005	B	B	A	ns	ns	ns	ns
	Gerreidae	ns	ns	ns	ns	0.0010	B	A	ns
	Mugilidae	0.0291	A	AB	B	0.0228	B	A	ns

Table 3

Results of Tukey's Post Hoc Multiple Comparisons for the larval position in the water column (Mid-Water vs Surface, Mid-Water vs Near Surface and Near Surface vs Surface) for each taxon and the three stations (West, centre and East; Fig 1). * marked at p-level < 0.005.

Taxa	Mean Diff.	Std. Err. Diff.	Lower CL	Upper CL	p-value
West					
Clupeidae					
Mid-Water *vs.* Surface	0.5888405	0.1471163	0.227847	0.9498336	0.0010*
Mid-Water *vs.* Near Surface	0.5533431	0.1471163	0.192350	0.9143362	0.0019*
Near Surface *vs.* Surface	0.0354974	0.1471163	-0.325496	0.3964905	0.9684
Cynoglossidae					
Mid-Water *vs.* Surface	0.2447095	0.0627611	0.090707	0.3987123	0.0013*
Mid-Water *vs.* Near Surface	0.2447095	0.0627611	0.090707	0.3987123	0.0013*
Near Surface *vs.* Surface	0.0000000	0.0627611	-0.154003	0.1540028	1.0000
Gerreidae					
Mid-Water *vs.* Surface	0.0795202	0.0964896	-0.157245	0.3162858	0.6909
Mid-Water *vs.* Near Surface	0.0704248	0.0964896	-0.166341	0.3071904	0.7477
Near Surface *vs.* Surface	0.0090954	0.0964896	-0.227670	0.2458610	0.9951
Mugilidae					
Mid-Water *vs.* Surface	0.2006867	0.0993886	-0.043192	0.4445658	0.1234
Mid-Water *vs.* Near Surface	0.1756008	0.0993886	-0.068278	0.4194800	0.1964
Near Surface *vs.* Surface	0.0250858	0.0993886	-0.218793	0.2689650	0.9655
Centre					
Clupeidae					
Mid-Water *vs.* Surface	0.7006627	0.1198522	0.406570	0.9947555	<.0001*
Mid-Water *vs.* Near Surface	0.6755768	0.1198522	0.381484	0.9696696	<.0001*
Near Surface *vs.* Surface	0.0250858	0.1198522	-0.269007	0.3191786	0.9762
Cynoglossidae					
Mid-Water *vs.* Surface	0.2300352	0.0824502	0.027719	0.4323511	0.0230
Mid-Water *vs.* Near Surface	0.1798635	0.0824502	-0.022452	0.3821794	0.0893
Near Surface *vs.* Surface	0.0501717	0.0824502	-0.152144	0.2524875	0.8165
Gerreidae					
Mid-Water *vs.* Surface	0.2053990	0.1182226	-0.084695	0.4954930	0.2067

Mid-Water *vs.* Near Surface	0.1032899	0.1182226	-0.186804	0.3933839	0.6604
Near Surface *vs.* Surface	0.1021091	0.1182226	-0.187985	0.3922031	0.6666
Mugilidae					
Mid-Water *vs.* Surface	0.4383711	0.1222035	0.138509	0.7382334	0.0030*
Mid-Water *vs.* Near Surface	0.4132853	0.1222035	0.113423	0.7131476	0.0052*
Near Surface *vs.* Surface	0.0250858	0.1222035	-0.274777	0.3249482	0.9771
East					
Clupeidae					
Mid-Water *vs.* Surface	0.5814190	0.1318111	0.257982	0.9048564	0.0003*
Mid-Water *vs.* Near Surface	0.5231715	0.1318111	0.199734	0.8466089	0.0010*
Near Surface *vs.* Surface	0.0582475	0.1318111	-0.265190	0.3816849	0.8983
Cynoglossidae					
Mid-Water *vs.* Surface	0.2834500	0.0698400	0.112077	0.4548230	0.0008*
Mid-Water *vs.* Near Surface	0.2834500	0.0698400	0.112077	0.4548230	0.0008*
Near Surface *vs.* Surface	0.0000000	0.0698400	-0.171373	0.1713730	1.0000
Gerreidae					
Mid-Water *vs.* Surface	0.3824772	0.1717873	-0.039053	0.8040078	0.0814
Mid-Water *vs.* Near Surface	0.2925454	0.1717873	-0.128985	0.7140761	0.2192
Near Surface *vs.* Surface	0.0899318	0.1717873	-0.331599	0.5114624	0.8604
Mugilidae					
Mid-Water *vs.* Surface	0.4269070	0.1625688	0.027997	0.8258174	0.0339*
Mid-Water *vs.* Near Surface	0.3790711	0.1625688	-0.019839	0.7779814	0.0652
Near Surface *vs.* Surface	0.0478359	0.1625688	-0.351074	0.4467463	0.9535

Table 4

Size range in standard length (mm), standard length means (mm) with standard deviation (SD) of the four taxa of fish larvae collected during ebb and flood conditions, and *p*-value statistic testing (Mann-Whitney U test) for differences in the standard-length distribution between ebb and flood conditions.

Taxa	Ebb			Flood			
	Min.	Max.	Mean (SD)	Min.	Max.	Mean (SD)	*p*-value
Clupeidae	11.25	22.40	14.02 (1.82)	11.88	22.38	13.82 (1.71)	0.0815
Cynoglossidae	10.10	12.48	11.09 (0.61)	9.30	12.68	10.79 (0.83)	0.0614
Gerreidae	4.17	7.08	5.50 (0.76)	3.08	7.08	5.20 (0.67)	0.0679
Mugilidae	7.71	19.17	10.51 (2.75)	6.25	22.80	10.38 (2.43)	0.7286